博士論文

Efficacy of the Novel Tubulin Polymerization Inhibitor PTC-028 for Myelodysplastic Syndrome

(骨髄異形成症候群における微小管阻害剤 PTC-028 の効果)

鐘　　丞

Abstract

Monomer tubulin polymerize into microtubules, which are highly dynamic and play a critical role in mitosis. Therefore, microtubule dynamics are an important target for anti-cancer drugs. The inhibition of tubulin polymerization or de-polymerization was previously targeted and exhibited efficacy against solid tumors. The novel small molecule PTC596 directly binds tubulin, inhibits microtubule polymerization, down-regulates MCL-1, and induces p53-independent apoptosis in acute myeloid leukemia cells. I herein investigated the efficacy of PTC-028, a structural analog of PTC596, in myelodysplastic syndrome (MDS). PTC-028 suppressed growth and induced apoptosis in MDS cell lines. The efficacy of PTC028 in primary MDS samples was confirmed using cell proliferation assays. PTC-028 synergized with hypomethylating agents, such as decitabine and azacitidine, to inhibit growth and induce apoptosis in MDS cells. Mechanistically, a treatment with PTC-028 induced G2/M arrest followed by apoptotic cell death. I also assessed the efficacy of PTC-028 in a xenograft mouse model of MDS using the MDS cell line, MDS-L and the AkaBLI bioluminescence imaging system, which is composed

of AkaLumine-HCl and Akaluc. PTC-028 prolonged the survival of mice in xenograft models. The present results suggest a chemotherapeutic strategy for MDS through the disruption of microtubule dynamics in combination with DNA hypomethylating agents.

Introduction

Myelodysplastic syndrome (MDS) is a type of hematological malignancy in which blood cells show dysplastic differentiation. This leads to the formation of dysfunctional blood cells in bone marrow (BM). Risk factors include previous chemotherapy or radiation therapy, exposure to heavy metals such as lead or mercury, and exposure to toxic chemicals such as benzene, pesticides, and tobacco smoke. In most cases, defective blood cells will be destroyed before leaving the BM and impaired hematopoiesis results in fewer blood cells. In some types of MDS, immature blood cells, called myeloblasts, increase in peripheral blood (PB) and BM. MDS patients will develop acute myeloid leukemia (AML) as the final stage if myeloblasts exceed the cut-off point of 20%.[1] The evolution process from normal stem cells to AML via MDS stage is shown below. (Figure 1) The signs and symptoms of MDS are generally associated with blood cytopenias; Anemia (reduced red blood cell count or low hemoglobin) may lead to shortness of breath, tingling sensation, chronic tiredness sometimes chest pain. Neutropenia (low neutrophil count) increases susceptibility

to infection. Patients who have thrombocytopenia (low platelet count) are subject to bleeding and bruising, as well as subcutaneous hemorrhaging resulting in purpura or petechiae.[2] Although MDS can be found in younger generations, most of the patients with MDS are above 60 years old.[3] The chromosome abnormalities such as chromosome 5q deletion (del(5q)) and monosomy 7 are often observed in patients with MDS.[4-5]

Prognosis of MDS patients can be assessed by various scoring systems; the International Prognostic Scoring System (IPSS) is the most common system now refined by the revised version (IPSS-R). Genomic information at baseline, which has not been included in clinical prognostic scores, will help us to stratify patients with various prognoses in the future. Therapy of MDS is based on risk stratification. The aim of therapy in low-risk MDS is to improve anemia or thrombocytopenia, decrease transfusion needs, improve quality of life, attempt to prolong overall survival, and reduce the risk of progression. In higher-risk MDS, the goal of therapy is to extend the lifespan of patients and reduce the risk of progression into acute leukemia. Previous research shows only a few drugs are currently available as the therapeutic agents; more drugs are now under clinical

investigation, in line with new, recently discovered molecular and immunological pathways.

Erythropoiesis stimulating agents (ESAs) are exploited to treat low-risk MDS (LR-MDS) patients with del(5q) showing low transfusion burden or symptomatic anemia.[6] However, many of these patients already have excessive EPO levels, which also correlate with a higher rate of clonal hematopoiesis of progenitor cells[7] and demonstrate a lack of response to ESAs. For these patients, who are also supported by continuous transfusion, lenalidomide is the option of treatment and results in erythroid response in more than 60% of patients.[8-10] The median response duration is 2 years. The MDS 004 study reveals that about 40% of the patients progressed to AML at 5 years.[10]

Interestingly, patients with a TP53 mutation have lower complete cytogenetic response to lenalidomide and were associated with a higher risk of leukemic transformation compared with patients having a wild-type TP53.[11]For this reason, patients diagnosed with del(5q) LR-MDS harboring or developing a TP53 mutation should be considered a distinct group requiring intensified disease surveillance, including assessment of clonal evolution of bone marrow sample. Data from the German MDS study group[12] support

that patients with TP53 mutation have a negative impact on survival and lower sensitivity to lenalidomide treatment. The size of the clone is also subject to change in some patients, featuring novel mutations during treatment but without an effect on outcome. Another study suggested that MDS patients with a lower TP53 mutation show a better outcome.[13] Other than TP53, disease progression is also observed in patients with *RUNX1* and *TET2* mutations.[14] Allo-HSCT or a potential clinical trial option can be the therapeutic strategy for patients failing lenalidomide with or without disease progression, whereas inhibition of DNA methyltransferases may be considered in the absence of any trial opportunity.[15]

DNA methyltransferases are the enzymes that catalyze addition of methyl group to DNA. There are three groups of methyltransferases – m6A, m4C and m5C methltransferases, which catalyze the reactions generating N6-methyladenine, N4-methylcytosine and C5-methylcytosine. In the process of many diseases like cancer, gene promoter CpG islands acquire abnormal hypermethylation, which results in transcriptional silencing that can be inherited by daughter cells following cell division.[16] Alterations of DNA methylation have been recognized as an important cause of cancer development. Hypomethylation, in general, arises earlier and plays a role in chromosomal instability and loss of imprinting,

whereas hypermethylation is observed at the promoter region and contribute to silencing of tumor suppressor genes. Therefore, targeting DNA hypermethylation might be a therapeutic strategy for cancer treatment.[17] The DNA hypomethylating agents decitabine and azacitidine are cytidine analogs and first-line drugs for the treatment of MDS. They may be incorporated into DNA and cause covalent binding with DNA methyltransferases, which prevent DNA synthesis and results in cytotoxicity. The inhibition of DNA methylation has extended the overall survival of patients with MDS and AML transformed from MDS.[15] Despite the administration of these chemotherapeutic agents, these diseases generally relapse and often become uncontrollable. Therefore, an innovative and more efficacious therapeutic strategy needs to be considered.

Microtubules are highly dynamic and involved in intracellular migration, cell movement, and mitosis. They play an important role in the attachment and segregation of chromosomes in various phases of cell division. Therefore, the targeting of microtubules represents a therapeutic strategy against both solid and hematological cancers.[18] The first approved microtubule-targeted agent (MTA) by the FDA was Vincristine (Figure 2), which has been clinically used to treat multiple types of cancers, particularly

hematological malignancies. The main side effects from vincristine treatment are chemotherapy-induced peripheral neuropathy, hair loss, constipation, and change in sensation. Severe peripheral neuropathy induced by vincristine may be a reason to restrict or avoid using the drug. The symptoms are tingling or numbness, pain and hypersensitivity to temperature, which start from the hands and feet and spread to the entire limbs.[19] One of the first symptoms of peripheral neuropathy is foot drop. Therefore, prescription of vincristine should be avoided for patients with a family history of hereditary motor and sensory neuropathy.[20] Nanoparticle albumin-bound paclitaxel or nab-paclitaxel was recently approved by FDA as the second MTA. In this formulation, paclitaxel (Figure 2) is bound to albumin as a delivery vehicle which increases the compound solubility and facilitates drug uptake into cancer cells. Clinically, Cremophor is utilized for solubilization of paclitaxel as a carrier agent, but additional significant toxicity of this agent is a problem for the patients. In contrast to Cremophor, nanoparticle albumin has prolonged stability and low toxicity in circulation. Previous research shows that drug delivery often fails in cancer cells due to poor perfusion and diffusion within the tumor parenchyma.[21] Therefore, it is desirable to develop novel agents against this

disease with low toxicity and prolonged stability. Indeed, in 2015, a positive phase III trial of nab-paclitaxel in combination with gemcitabine led to its approval for use in metastatic pancreatic cancer.[22]

Over the past few decades, additional MTAs have been developed and received FDA approval, mostly for applications to cancer therapies. These agents have been classified by their binding sites on tubulin, which influences their roles in the inhibition or stabilization of polymerized microtubules. The novel small molecule PTC596 directly binds tubulin and inhibits microtubule polymerization.[23] PTC596 was originally developed to target BMI1-positive cancer stem cells. BMI1 protein is a component of polycomb repressive complex 1 that maintains the transcriptional repression of target genes via ubiquityl histone H2A.[24-26] PTC596 was recently identified as a direct microtubule polymerization inhibitor in a preclinical study on pancreatic ductal adenocarcinoma and its function as a BMI1 modulator was shown to be a secondary effect.[23] PTC596 induces cytotoxicity in various tumor cell lines and exerts preclinical effects on hematological malignancies, such as AML, mantle cell leukemia, and multiple myeloma.[24-26] Clinical trials on PTC596 are ongoing for diffuse intrinsic pontine glioma,

leiomyosarcoma, and ovarian cancer. (ClinicalTrials.gov Identifiers: NCT03605550, NCT03761095, and NCT03206645). PTC-028 has also been characterized as a BMI1 modulator that has therapeutic potential in ovarian cancer, endometrial cancer, and medulloblastoma.[27-29] PTC-028 selectively decreases cancer cell proliferation whereas normal cells remain unaffected. The molecular mechanism suggests that PTC-028 induces BMI-1 degradation through protein phosphorylation and activates intracellular apoptotic pathway. However, it has been reported that PTC596 induces microtubule depolymerization and exhibits cytotoxic activity independent of BMI1.[23, 26] The finding suggests that PTC-028 may function as an inhibitor of tubulin assembly.

In this study, I investigated the efficacy of PTC-028 in MDS and found its role as a microtubule polymerization inhibitor that synergizes with hypomethylating agents to inhibit growth and induce apoptosis in MDS cells.

Materials and Methods

Cell culture and drug treatment

The HL-60, THP-1, and MOLM-13 cell lines were acquired from ATCC. The TF-1 cell line was provided by Toshio Kitamura (The University of Tokyo, Japan). The SKM-1 and SKK-1 cell lines were provided by Dr. Hiroshi Matsuoka (Kobe University, Japan). Cells were maintained in RPMI-1640 supplemented with 10% fetal bovine serum (FBS) (Sigma-Aldrich) and 1% penicillin/streptomycin (Gibco). SKM-1 cells were cultured in RPMI supplemented with 20% FBS. MDS-L cells[30-34] were cultured in the presence of human IL-3 (10 ng/ml) (BioLegend). TF-1 and SKK-1 were cultured in the presence of 1 and 10 ng/ml of GM-CSF (1 ng/ml) (BioLegend), respectively. Stocks of PTC-028 (synthesized for PTC Therapeutics) and decitabine (Wako) were prepared in DMSO (Sigma-Aldrich) at concentrations of 3 and 10 mM, respectively. In growth assays, cells were seeded on 24-well plates at 1×10^5 cells/ml in triplicate and treated with graded concentrations of PTC-028 and decitabine. Cells were counted using 0.1% trypan blue dye. MTS viability tests were conducted according to the manufacturer's instructions

(Promega). Synergism was assessed by calculating the proportion of cell growth using CompuSyn software (ComboSyn, Inc.).[35]

Apoptosis and cell cycle assays

Apoptosis and the cell cycle were examined using an Annexin V Apoptosis kit and BrdU Flow kit (BD Pharmingen) according to the manufacturer's instructions. Flow cytometric analyses were performed on BD FACS Celesta (BD Bioscience).

RNA sequencing

Total RNA was isolated from MDS-L and SKM-1 cells treated with DMSO or 30 nM of PTC-028 using the RNeasy Mini Kit (Qiagen). After reverse transcription, the libraries for RNA-seq were generated from fragmented DNA with 15 cycles of amplification using a NEB Next Ultra DNA Library Prep Kit (New England BioLabs). After the libraries had been quantified using TapeStation (Agilent), samples were subjected to sequencing with Hiseq2500 (Illumina) and 61 cycles of sequencing reactions were performed. RNA-seq raw reads (fastq files) were mapped to a human genome. Gene level counts for fragments

mapping uniquely to the human genome were extracted from BAM files. Gene expression values were then calculated as reads per kilobase of exon units per million mapped reads (RPKM) using cufflinks (version 2.2.1). A gene set enrichment analysis (GSEA) was performed based on curated gene sets from the Broad Institute's molecular signatures database MSigDB.

Deposition of data

RNA sequence data were deposited in the DNA Data Bank of Japan (DDBJ) (accession number DRA10205).

AkaBLI system

In vivo bioluminescence imaging (BLI) is a non-invasive method for measuring light output produced by the enzyme-catalyzed oxidation reaction of a substrate. The AkaBLI system, composed of AkaLumine-HCl and Akaluc, provides a light source of sufficient strength to penetrate body walls, even in deep tissue areas.[36] pcDNA3/Venus-Akaluc was obtained from the RIKEN BioResource Research Center (Catalog No: RDB15781). The

nucleotide sequence of the synthetic construct Akaluc gene for the firefly luciferase mutant protein Akaluc is available under DDBJ accession No: LC320664. Regarding the generation of the CS-CDF-UbC-mScarlet-P2A-Akaluc-PRE lentiviral vector, mScarlet (synthesized by FASMAC Co., Ltd., Japan) and Akaluc CDS were cloned into the CS-CDF-UbCG-PRE lentiviral vector (Catalog No: RDB08363, a gift from Dr. H. Miyoshi) downstream of the ubiquitin C promoter (UbC) using the AgeI and XhoI restriction sites, replacing the existing GFP CDS. Cloning primers were designed to include an in-frame addition of the GSG-P2A self-cleaving peptide sequence between the mScarlet and Akaluc sequences.

Lentiviral production and transduction

A recombinant mScarlet-P2A-Akaluc lentivirus (LV) was generated by the transient co-transfection of HEK293T cells with CS-CDF-UbC-mScarlet-2A-Akaluc-PRE and the helper plasmids pMD2.G (Addgene #12259) and psPAX2 (Addgene #12260) using the polyethylenimine (PEI) method. Culture supernatants were collected after 96 hours and

filtered (22 μm), followed by the concentration of LV particles by centrifugation at 40000 *g* for 4 hours.

Xenograft studies

All studies involving animals were performed in accordance with the institutional guidelines for the use of laboratory animals and approved by the Review Board for Animal Experiments of the University of Tokyo (approval ID PA18-42). NOD.Cg-Prkdc^{scid} Il2rg^{tm1Sug} Tg (SRa-IL3, CSF2)/Jic (NOG IL-3/GM-Tg) mice expressing human IL-3 and GM-CSF were purchased from the Central Institute for Experimental Animals (Kawasaki Japan).[33] MDS-L/Akaluc cells (1×10^7 cells) were inoculated into female NOG IL-3/GM-TG mice[37] irradiated at a dose of 1.8 Gy. Three weeks after tumor inoculation, mice were randomly divided into three groups (6 mice per group) and treated with the indicated compounds. One hundred microliters of 5 mM AkaLumine-HCl (Wako) was injected intraperitoneally into mice just before the imaging analysis and mice under isoflurane anesthesia were imaged within 5 to 10 minutes of the injection. The following conditions were used for image acquisition: open for total bioluminescence, exposure

time = 60 sec, binning = 4 to 8, field of view = 25 × 25 cm, and f/stop = 1. *In vivo* photon counting was conducted with an IVIS system using Living Image 2.5 software (Xenogen). Mice were monitored until they became moribund, at which time they were euthanized.

Primary MDS samples

Freshly isolated primary MDS cells were obtained from the BM aspirates of 1 patient with MDS and 1 with MDS/AML. All patients provided written informed consent according to institutional guidelines. The present study was approved by the Institutional Review Board at the University of Tokyo and Chiba University (approval #30-47-B1002 and #844, respectively). BM-MNCs were isolated using LymphoPrep (Cosmo Bio) and $CD34^+$ cells were obtained from BM-MNCs using a CD34 MicroBead kit (Miltenyi Biotec). $CD34^+$ cells were seeded into culture flasks in RPMI medium supplemented with 1% penicillin/streptomycin, 20% FBS, and 10 ng/ml of SCF, TPO, IL-3, GM-CSF, and FLT3 ligand (BioLegend). The effects of PTC-028 and decitabine in combination were evaluated using the MTS viability test (Promega).

Immunoblot analysis of tubulin in MDS cells

MDS-L cells were cultured in the presence of PTC-028 for 4 hours. Cells were washed with PBS, permeabilized with 200 μl of pre-warmed buffer [80 mM PIPES-KOH (pH 6.8), 1 mM $MgCl_2$, 1 mM EGTA, 0.2% Triton X-100, 10% glycerol, and 1 × Protease inhibitor], and incubated at 30°C for 5 min. Supernatants containing the soluble fraction of microtubules were separated after centrifugation, mixed with 4 × Laemmli gel sample buffer, and boiled for 3 min. To collect the insoluble polymerized tubulin fraction, 250 μl of 1 × Laemmli gel sample buffer was added to the pellet, followed by boiling for 3 min. Microtubules were detected by Western blotting and probed with mouse anti-human α-tubulin antibodies.

Statistical analysis

Data are shown as the mean ± SD or SEM. In statistical analyses, p-values were derived using unpaired Student's *t*-tests for any studies with only two groups. Otherwise, comparisons of groups were performed on log-transformed data using a one-way ANOVA test. Survival curves were calculated by the Kaplan-Meier method and

compared using the Log-rank test. All analyses were conducted using GraphPad Prism Software.

Results

PTC-028 disrupts tubulin integrity in MDS cells.

PTC-028 is a novel derivative of PTC596, which was recently shown to directly inhibit microtubule polymerization in pancreatic ductal adenocarcinoma cells (Figure 3).[23] I first investigated the effects of PTC-028 on the levels of soluble (unpolymerized) versus polymerized tubulin in MDS-L cells. Cells were treated with PTC-028 (3 and 5 μM) and paclitaxel (1 μM) for 4 hours[38], and cell lysates were then separated into soluble and polymerized fractions by centrifugation. The visualization of tubulin fractions by Western blotting demonstrated that the PTC-028 treatment for 4 hours resulted in the near-complete loss of polymerized microtubules (Figure 4). In contrast, polymerized microtubules increased in cells treated with Paclitaxel, which stabilizes microtubules against depolymerization (Figure 4).[39] These results indicate that PTC-028 also acts as a microtubule polymerization inhibitor.

PTC-028 inhibits cell growth and induces apoptosis in MDS cell lines.

A previous study reported that PTC596 suppressed cell proliferation and induced apoptosis in AML cell lines.[24] Since MDS is regarded as a pre-leukemic stage, I examined the effects of PTC-028 on MDS cells. MDS-L is a subline derived from the human MDS cell line, MDS92 established from the BM of an MDS patient.[30-33] This cell line has complex karyotypic abnormalities, including del(5q) [der(5)(5;19)], monosomy 7, and somatic mutations in *NRAS* and *TP53*, and a *HIST1H3C* mutation (histone H3 K27M).[33] SKM-1 is a cell line derived from a patient with MDS/AML, which has no chromosomal abnormalities, but has point mutations in *NRAS* and *KRAS*.[40] I also used the MDS/AML cell lines, TF-1,[41] MOLM-13,[42] and SKK-1,[43] and AML cell lines, HL-60 and THP-1. PTC-028 induced the dose-dependent inhibition of cell proliferation on both MDS and AML cells (Figure 5). Cell proliferation detected by MTS assays revealed that MDS cells were sensitive to PTC-028, as demonstrated by the low concentrations of PTC-028 needed to inhibit cell viability by 50% (cytotoxic concentration; CC_{50}); however, MDS-L, SKM-1, and TF-1 were less sensitive than others (Figure 6). I isolated $CD34^+$ cells from primary MDS BM samples and investigated the efficacy of PTC-028 on primary MDS cells. Patient characteristics are shown in Table 1. Cell growth at 48 hours in culture

was examined by MTS assays and the counting of viable cells. The growth inhibitory effects of PTC-028 were confirmed in primary MDS cells (Figure 7). I then performed apoptosis assays. Caspase 3/7 activities were significantly induced in MDS cells in the presence of PTC-028 (Figure 8), suggesting the induction of apoptotic cell death by PTC-028.

Combination of PTC-028 and DNA hypomethylating agents exerts synergistic effects

To enhance the therapeutic benefits of PTC-028 on MDS cells, I investigated synergism between PTC-028 and DNA hypomethylating agents. I treated MDS-L and SKM-1 cells with increasing concentrations of PTC-028 in combination with DNA hypomethylating agents, first-line therapeutic agents in the treatment of MDS. After 3 days of culture, cell growth was analyzed by MTS assays. I then calculated the combination index (CI) that defines effect quantitatively: additive (CI=1), synergistic (CI<1), and antagonistic (CI>1) effects in drug combinations.[35] PTC-028 and decitabine exerted synergistic cytotoxic effects at most concentrations tested, showing a very low CI, although the effect was

rather additive at some concentrations (Figure 9). Azacitidine was also effective in combination with PTC-028 (Figure 9). Apoptosis assays using Annexin V revealed that PTC-028 and DNA hypomethylating agents both significantly induced apoptosis in MDS-L cells as single agents as well as in combination therapy (Figure 10). I then investigated PTC596 on the growth of MDS cells. PTC596 inhibited the growth of MDS-L cells and showed moderate synergism when combined with decitabine (Figure 11 and 12). The CC_{50} values of PTC596 in MDS and AML cells were moderately higher than those of PTC-028 (Figure 13), indicating that PTC-028 exerts a better cytotoxic effect than PTC596. I next tested the efficacy of clinically used agents targeting microtubule such as Vincristine and Paclitaxel. The CC50 value of PTC-028 was lower than those of Vincristine and Paclitaxel (Figure 13). The data indicate that PTC-028 is a more effective therapeutic agent for MDS therapy.

PTC-028 induces mitotic arrest and changes gene expression in MDS cells

To clarify the mechanisms by which PTC-028 plays a role in the cell cycle, I performed BrdU cell cycle assays. The results obtained clearly showed that PTC-028 induced the

accumulation of cells at the G2/M phase (Figure 14). The disruption of tubulin assembly was previously shown to induce mitotic arrest in cancer cells.[44-46]

I next investigated the effects of PTC-028 on the transcriptome, I performed an RNA-seq analysis of MDS-L and SKM-1 cells treated with PTC-028. In total, 163 and 404 genes and 39 and 82 genes were up- (≥1.5-fold) and down-regulated (≤ 0.6-fold) in MDS-L and SKM-1 cells, respectively, upon the PTC-028 treatment (Figure 15). GSEA of RNA-seq data revealed that MYC and E2F target gene sets were negatively enriched with significance in PTC-028-treated MDS-L and SKM-1 cells (Figure 16, Table 2-5). In contrast, apoptosis gene sets were positively enriched in PTC-028-treated cells (Figure 16, Table 2-5). These results were consistent with growth inhibition and enhanced apoptosis by PTC-028. Previous studies reported the activation of NF-κB and inflammatory signaling pathway by microtubule inhibitors.[47-48] PTC-028 also activated gene sets in the downstream of following pathways: TNFα signaling via NFκB and inflammatory response (Figure 16).

PTC-028 exerts therapeutic efficacy in the xenograft MDS model

I assessed the efficacy of PTC-028 in a xenograft mouse model of MDS. To precisely monitor the tumor burden in mice, we took advantage of the AkaBLI system, composed of AkaLumine-HCl and Akaluc, which improved performance by a factor of 100 to 1,000 over the conventional bioluminescence imaging system composed of luciferin and luciferase.[36] MDS-L cells were transduced with the Akaluc gene using a recombinant mScarlet-P2A-Akaluc lentivirus and selected by mScarlet expression as a marker. MDS-L/Akaluc cells (1×10^7) were intravenously inoculated into NOG mice (NOG IL-3/GM TG)[33] irradiated at a dose of 1.8 Gy. The tumor burden was monitored by bioluminescence signals in *in vivo* imaging assays. MDS-L cells, which retain MDS-like features, expanded very slowly in NOG IL-3/GM-TG mice and induced lethal disease after a long latency. Recipient mice were treated with PTC-028 for 7 weeks (Figure 17). PTC-028 significantly inhibited the growth of MDS-L cells and prolonged the overall survival of recipient mice (Figure 18-20). Furthermore, the combination therapy of PTC-028 and DAC significantly reduced the tumor burden compared to PTC-028 or DAC alone (Figure 21-22) and significantly prolonged the overall survival of recipient mice (Figure 23). Mice that received combination therapy showed moderate weight loss 11 days after the

initiation of the treatment, but subsequently recovered (Figure 24). Hemoglobin levels in the PB of mice did not significantly change during combination therapy (Figure 24).

Discussion

MTAs are categorized into two major groups: stabilizing and depolymerizing agents. Microtubule-stabilizing agents, including paclitaxel and docetaxel, operate by increasing polymerization and the tubulin polymer mass in cells. Depolymerizing agents, such as vincristine and vinblastine, inhibit polymerization, induce microtubule degradation, and decrease polymer mass. However, at the lowest effective concentrations, both stabilizers and depolymerizing agents induce suppression of microtubule dynamics without changing polymer mass. As the action of MTAs become clear at the molecular level, differences in mechanisms of action of these agents are being elucidated. These differences may be dependent on the observed disparities in activity such as the binding sites of MTAs; the taxan site is the primary binding domain of microtubule-stabilizing agents whereas depolymerizing agents bind to vinca and colchicine domain.

In this study, I demonstrated the activities of a novel MTA PTC-028 alone or in combination with decitabine in MDS both *in vitro* and *in vivo*. Although PTC-028 has been reported as a BMI-1 inhibitor,[27-29] I confirmed the inhibitory effect of PTC-028 on tubulin polymerization. PTC-028-induced G2/M cell cycle arrest may be attributed to the

microtubule depolymerization by PTC-028. BMI-1 plays an essential role in MDS cell progression, survival, and drug resistance[49-50]. PTC-028 has been shown to decrease BMI-1 protein and H2A mono-ubiquitination levels in medulloblastoma and ovarian cancer cell lines[27, 29]. My data also indicate modest reduction of BMI-1 in MDS-L. (Figure 25) The underlying pharmacological mechanism involved PTC-028 inducing a reduction in BMI-1 via phosphorylation at the protein level[14]. However, BMI-1 is known to be hyperphosphorylated and dissociates from chromatin during mitosis[51]. Since PTC-028 induces mitotic cell arrest, these findings suggest that BMI-1 degradation mediated by PTC-028 is a secondary response.

PTC-028 significantly induced cytotoxicity in MDS cell lines, primary MDS cells, and MDS cells in a xenograft model. Our data show preclinical efficacy of PTC-028 as a therapeutic strategy for MDS. DNA hypomethylating agents are the first choice for treatment of MDS. A previous study reported that decitabine induced DNA damage, G2/M arrest and caspase-mediated apoptosis. I found that the combination treatment of PTC-028 and decitabine or azacitidine exhibited synergistic efficacy in MDS cells. My *in vivo* results obtained using the xenograft model revealed that this combination is

promising, with a definitive synergy and acceptable tolerability. Therefore, I demonstrated that PTC-028 combined with DNA hypomethylating agents is an effective strategy for MDS therapy.

Similar to other microtubule-destabilizing agents, PTC-028 induces MDS cell apoptosis. Since the dynamic behavior of microtubule is essential for mitosis, apoptosis induced by microtubule-destabilizing agents is often attributed to the dissolution of mitotic spindles and mitotic arrest. However, the effects of microtubule-destabilizing agents on the microtubule network extend beyond the ability to halt cells in mitosis and include the induction of apoptosis at all phases of the cell cycle, even in non-cycling cells.[18] Acute cell cycle-independent apoptosis in response to microtubule-destabilizing agents has been reported in hematopoietic cells and involves several pathways that dysregulate Bcl-2 family proteins.[18] Further studies are needed to evaluate whether PTC-028 exerts similar effects to other drugs.

Vincristine is a chemotherapy drug used to treat several different types of cancer. The chemotherapeutic agent belongs to a group of drugs called vinca alkaloids. The drug stops the cancer cell proliferation and causes mitotic arrest. Moreover, vincristine is combined

with other agents like cytarabine and pirarubicin for treatment of AML patients with Down syndrome; the five-year overall survival rate is also high.[52] The study suggests the possibility of using microtubule inhibitors to treat hematological malignancies. My data indicate the lower cc50 of PTC-028, which might be attributed to BMI-1 degradation. Therefore, PTC-028 may have a better efficacy than vincristine when tested in the clinical trial.

The GSEA analysis showed an up-regulated inflammatory response and apoptosis after the treatment with PTC-028. The relationship between inflammation and cell death has been reported in previous studies[53-54]. The release of intracellular material from dead cells triggers inflammatory reactions, including the activation of the NF-κB pathway[54]. However, another mechanism shows that the disruption of microtubule dynamics induces the nuclear translocation of NF-κB via IκB degradation[55-56]. Collectively, these findings explain the enrichment of gene sets targeted by inflammatory responses and the NF-κB signaling pathway. Since the inflammatory cytokines produced through the activation of NF-κB signaling recruit immune cells, which trigger anti-cancer immunity, MDS cells may also be eliminated by immune activation via PTC-028-induced inflammatory

responses.

In conclusion, the present results demonstrate that the inhibition of microtubule polymerization alone and in combination with DNA hypomethylating agents has the potential as a novel therapeutic strategy for MDS. The present study provides a preclinical framework for the clinical evaluation of this promising therapeutic approach to improve outcomes in MDS patients.

Acknowledgments

I would like to express my sincere thanks to my supervisor Prof. Atsushi Iwama for his support throughout my research work. His guidance was paramount during this project. I am also grateful to Dr. Kensuke Kayamori for his helpful advice on my experiments. I would like to thank Dr. Shuhei Koide for his technical support and Dr. Motohiko Oshima for data analysis. I also thank PTC therapeutics for providing PTC-028 and PTC596. I was also blessed with many researchers who gave me materials necessary for my research. I would like to thank Dr. Satoshi Yamazaki (The University of Tokyo, Japan), Dr. Satoshi Iwano (RIKEN, Saitama, Japan) Dr. Toshio Kitamura (The University of Tokyo, Japan) and Dr. Hiroshi Matsuoka (Kobe University, Japan), for providing Akaluc vector and cell lines. Lastly, I would like to show my gratitude to my family members for their love and support.

References

1. Corey SJ, Minden MD, Barber DL, Kantarjian H, Wang JC, Schimmer AD. Myelodysplastic syndromes: the complexity of stem-cell diseases. Nat Rev Cancer. 2007;7:118-29.

2. Desborough M, Estcourt LJ, Chaimani A, Doree C, Hopewell S, Trivella M, Hadjinicolaou AV, Vyas P, Stanworth SJ. Alternative agents versus prophylactic platelet transfusion for preventing bleeding in patients with thrombocytopenia due to chronic bone marrow failure: a network meta-analysis and systematic review. Cochrane Database Syst Rev. 2016 Jan 26; 2016(1): CD012055.

3. Ma X. Epidemiology of Myelodysplastic Syndromes. Am J Med. 2012 Jul; 125.

4. Vera Adema and Rafael Bejar. What lies beyond del(5q) in myelodysplastic syndrome? Haematologica. 2013 Dec; 98(12): 1819–1821

5. Dilek Aktas, Ergul Tuncbilek. Myelodysplastic syndrome associated with monosomy 7 in childhood: a retrospective study. Cancer Genet Cytogenet. 2006 Nov; 171(1): 72-5.

6. Hellstrom-Lindberg E, Gulbrandsen N, ¨ Lindberg G, Ahlgren T, Dahl IMS, Dybedal I, Grimfors G, Hesse-Sundin E, Hjorth M, Kanter-Lewensohn L, Linder O, Luthman

M, Löfvenberg E, Oberg G, Porwit-MacDonald A, Rådlund A, Samuelsson J, Tangen JM, Winquist I, Wisloff F. A validated decision model for treating the anaemia of myelodysplastic syndromes with erythropoietin 1 granulocyte colonystimulating factor: significant effects on quality of life. Br J Haematol. 2003;120(6):1037-1046.

7. Oelschlaegel U, Alexander Rohnert M, Mohr B, Sockel K, Herold S, Ehninger G, Bornhäuser M, Thiede C, Platzbecker U. Clonal architecture of del(5q) myelodysplastic syndromes: aberrant CD5 or CD7 expression within the myeloid progenitor compartment defines a subset with high clonal burden. Leukemia. 2016;30(2):517-520.

8. Giagounidis AAN, Kulasekararaj A, Germing U, Radkowski R, Haase S, Petersen P, Göhring G, Büsche G, Aul C, Mufti GJ, Platzbecker U. Long-term transfusion independence in del(5q) MDS patients who discontinue lenalidomide. Leukemia. 2012;26(4):855-858.

9. Giagounidis A, Mufti GJ, Mittelman M, Sanz G, Platzbecker U, Muus P, Selleslag D, Beyne-Rauzy O, te Boekhorst P, del Cañizo C, Guerci-Bresler A, Nilsson L, Lübbert M, Quesnel B, Ganser A, Bowen D, Schlegelberger B, Göhring G, Fu T, Benettaib B, Hellström-Lindberg E, Fenaux P. Outcomes in RBC transfusion-dependent patients with low-/intermediate-1-risk myelodysplastic syndromes with isolated deletion 5q treated with lenalidomide: a subset analysis from the MDS-004 study. Eur J Haematol. 2014;93(5):429-438.

10. Fenaux P, Giagounidis A, Selleslag D, Beyne-Rauzy O, Mufti G, Mittelman M, Muus P, Te Boekhorst P, Sanz G, Del Cañizo C, Guerci-Bresler A, Nilsson L, Platzbecker U, Lübbert M, Quesnel B, Cazzola M, Ganser A, Bowen D, Schlegelberger B, Aul C, Knight R, Francis J, Fu T, Hellström-Lindberg E; MDS-004 Lenalidomide del5q Study Group. A randomized phase 3 study of lenalidomide versus placebo in RBC transfusion-dependent patients with Low-/Intermediate-1-risk myelodysplastic syndromes with del5q. Blood. 2011;118(14):3765-3776.

11. Jadersten M, Saft L, Smith A, Kulasekararaj A, Pomplun S, Göhring G, Hedlund A, Hast R, Schlegelberger B, Porwit A, Hellström-Lindberg E, Mufti GJ. TP53 mutations in low-risk myelodysplastic syndromes with del(5q) predict disease progression. J Clin Oncol. 2011;29(15): 1971-1979.

12. Mossner M, Jann JC, Nowak D, Platzbecker U, Giagounidis A, Götze K, Letsch A, Haase D, Shirneshan K, Braulke F, Schlenk RF, Haferlach T, Schafhausen P, Bug G, Lübbert M, Ganser A, Büsche G, Schuler E, Nowak V, Pressler J, Obländer J, Fey S, Müller N, Lauinger-Lörsch E, Metzgeroth G, Weiß C, Hofmann WK, Germing U, Nolte F. Prevalence, clonal dynamics and clinical impact of TP53 mutations in patients with myelodysplastic syndrome with isolated deletion (5q) treated with lenalidomide: results from a prospective multicenter study of the german MDS study group (GMDS). Leukemia. 2016;30(9):1956-1959.

13. Sallman DA, Komrokji R, Vaupel C, Cluzeau T, Geyer SM, McGraw KL, Al Ali NH, Lancet J, McGinniss MJ, Nahas S, Smith AE, Kulasekararaj A, Mufti G, List A, Hall

J, Padron E. Impact of TP53 mutation variant allele frequency on phenotype and outcomes in myelodysplastic syndromes. Leukemia. 2016; 30(3):666-673.

14. Scharenberg C, Giai V, Pellagatti A, Saft L, Dimitriou M, Jansson M, Jädersten M, Grandien A, Douagi I, Neuberg DS, LeBlanc K, Boultwood J, Karimi M, Jacobsen SE, Woll PS, Hellström-Lindberg E. Progression in patients with low- and intermediate-1-risk del(5q) myelodysplastic syndromes is predicted by a limited subset of mutations. Haematologica. 2017;102(3): 498-508

15. Platzbecker U. Treatment of MDS. Blood. 2019;133:1096-107.

16. Wang YP, Lei QY. Metabolic recoding of epigenetics in cancer. Cancer Communications. 2018; 38 (1): 25.

17. Daura-Oller E, Cabre M, Montero MA, Paternain JL, Romeu A. Specific gene hypomethylation and cancer: new insights into coding region feature trends. Bioinformation. 2009; 3 (8): 340–343

18. Bates D, Eastman A. Microtubule destabilising agents: far more than just antimitotic anticancer drugs. Br J Clin Pharmacol. 2017;83:255-68.

19. Chemotherapy-induced Peripheral Neuropathy. NCI Cancer Bulletin. Feb 23, 2010 [archived 2011-12-11];7(4):6.

20. Graf WD, Chance PF, Lensch MW, Eng LJ, Lipe HP, Bird TD. Severe vincristine neuropathy in Charcot-Marie-Tooth disease type 1A Cancer. 1996. **77** (7): 1356–62

21. Olive KP, Jacobetz MA, Davidson CJ, Gopinathan A, McIntyre D, Honess D, Madhu B, Goldgraben MA, Caldwell ME, Allard D, Frese KK, Denicola G, Feig C, Combs C, Winter SP, Ireland-Zecchini H, Reichelt S, Howat WJ, Chang A, Dhara M, Wang L, Rückert F, Grützmann R, Pilarsky C, Izeradjene K, Hingorani SR, Huang P, Davies SE, Plunkett W, Egorin M, Hruban RH, Whitebread N, McGovern K, Adams J, Iacobuzio-Donahue C, Griffiths J, Tuveson DA. Inhibition of Hedgehog signaling enhances delivery of chemotherapy in a mouse model of pancreatic cancer. Science 2009; 324:1457–61.

22. Von Hoff DD, Ervin T, Arena FP, Chiorean EG, Infante J, Malcolm Moore M, Seay T, Tjulandin SA, Ma WW, Saleh MN, Harris M, Reni M, Dowden S, Laheru D, Bahary N, Ramanathan RK, Tabernero J, Hidalgo M, Goldstein D, Van Cutsem E, Wei X, Iglesias J, Renschler MF. Increased survival in pancreatic cancer with nab-paclitaxel plus gemcitabine. N Engl J Med 2013;369:1691–703.

23. Eberle-Singh JA, Sagalovskiy I, Maurer HC, Sa.stra SA, Palermo CF, Decker AR, Kim MJ, Sheedy J, Mollin A, Cao L, Hu J, Branstrom A, Weetall M, Olive KP. Effective delivery of a microtubule polymerization inhibitor synergizes with standard regimens in models of pancreatic ductal adenocarcinoma. Clin Cancer Res. 2019;25:5548-60.

24. Nishida Y, Maeda A, Kim MJ, Cao L, Kubota Y, Ishizawa J, AlRawi A, Kato Y, Iwama A, Fujisawa M, Matsue K, Weetall M, Dumble M, Andreeff M, Davis TW, Branstrom A, Kimura S, Kojima K. The novel BMI-1 inhibitor PTC596 downregulates MCL-1 and induces p53-independent mitochondrial apoptosis in acute myeloid leukemia progenitor cells. Blood Cancer J. 2017;7: e527.

25. Maeda A, Nishida Y, Weetall M, Cao L, Branstrom A, Ishizawa J, Nii T, Schober WD, Abe Y, Matsue K, Yoshimura M, Kimura S, Kojima K. Targeting of BMI-1 expression by the novel small molecule PTC596 in mantle cell lymphoma. Oncotarget. 2018;9:28547-60.

26. Bolomsky A, Muller J, Stangelberger K, Lejeune M, Duray E, Breid H, Vrancken L, Pfeiffer C, Hübl W, Willheim M, Weetall M, Branstrom A, Zojer N, Caers J, Ludwig H. The anti-mitotic agents PTC-028 and PTC596 display potent activity in pre-clinical models of multiple myeloma but challenge the role of BMI-1 as an essential tumour gene. Br J Haematol. 2020 Sep;190(6):877-890.

27. Dey A, Xiong X, Crim A, Dwivedi SKD, Mustafi SB, Mukherjee P, et al. Evaluating the mechanism and therapeutic potential of PTC-028, a novel inhibitor of BMI-1 function in ovarian cancer. Mol Cancer Ther. 2018;17:39-49.

28. Buechel M, Dey A, Dwivedi SKD, Crim A, Ding K, Zhang R, Mukherjee P, Moore KN, Cao L, Branstrom A, Weetall M, Baird J, Bhattacharya R. Inhibition of BMI1, a therapeutic approach in endometrial cancer. Mol Cancer Ther. 2018;17:2136-43.

29. Bakhshinyan D, Venugopal C, Adile AA, Garg N, Manoranjan B, Hallett R, Wang X, Mahendram S, Vora P, Vijayakumar T, Subapanditha M, Singh M, Kameda-Smith MM, Qazi M, McFarlane N, Mann A, Ajani OA, Yarascavitch B, Ramaswamy V, Farooq H, Morrissy S, Cao L, Sydorenko N, Baiazitov R, Du W, Sheedy J, Weetall M, Moon YC, Lee CS, Kwiecien JM, Delaney KH, Doble B, Cho YJ, Mitra S, Kaplan D, Taylor MD, Davis TW, Singh SK. BMI1 is a therapeutic target in recurrent medulloblastoma. Oncogene. 2019;38:1702-16.

30. Yanagihara K, Takigahira M, Takeshita F, Komatsu T, Nishio K, Hasegawa F, Ochiya T. A photon counting technique for quantitatively evaluating progression of peritoneal tumor dissemination. Cancer Res. 2006;66(15):7532-7539.

31. Drexler HG, Dirks WG, Macleod RA. Many are called MDS cell lines: one is chosen. Leuk Res. 2009;33(8):1011-1016.

32. Matsuoka A, Tochigi A, Kishimoto M, Nakahara T, Kondo T, Tsujioka T, Tasaka T, Tohyama Y, Tohyama K. Lenalidomide induces cell death in an MDS-derived cell line with deletion of chromosome 5q by inhibition of cytokinesis. Leukemia. 2010;24(4):748-755.

33. Tohyama K, Tsutani H, Ueda T, Nakamura T, Yoshida Y. Establishment and characterization of a novel myeloid cell line from the bone marrow of a patient with the myelodysplastic syndrome. Br J Haematol. 1994;87(2):235-242.

34. Kida JI, Tsujioka T, Suemori SI, Okamoto S, Sakakibara K, Takahata T, Yamauchi T, Kitanaka A, Tohyama Y, Tohyama K. An MDS-derived cell line and a series of its sublines serve as an in vitro model for the leukemic evolution of MDS. Leukemia. 2018;32(8):1846-1850.

35. Chou TC. Drug combination studies and their synergy quantification using the Chou-Talalay method. Cancer Res. 2010;70(2):440-446.

36. Iwano S, Sugiyama M, Hama H, Watakabe A, Hasegawa N, Kuchimaru T, Kuchimaru T, Tanaka KZ, Takahashi M, Ishida Y, Hata J, Shimozono S, Namiki K, Fukano T, Kiyama M, Okano H, Kizaka-Kondoh S, McHugh TJ, Yamamori T, Hioki H, Maki S, Miyawaki A. Single-cell bioluminescence imaging of deep tissue in freely moving animals. Science. 2018;359(6378):935-939.

37. Ito R, Takahashi T, Katano I, Kawai K, Kamisako T, Ogura T, Ida-Tanaka M, Suemizu H, Nunomura S, Ra C, Mori A, Aiso S, Ito M. Establishment of a human allergy model using human IL-3/GM-CSF-transgenic NOG mice. J Immunol. 2013;191(6):2890-2899.

38. Punganuru SR, Madala HR, Mikelis CM, Dixit A, Arutla V, Srivenugopal KS. Conception, synthesis, and characterization of a rofecoxib-combretastatin hybrid drug with potent cyclooxygenase-2 (COX-2) inhibiting and microtubule disrupting activities in colon cancer cell culture and xenograft models. Oncotarget 2018 May

25;9(40):26109-26129.

39. Rowinsky, E. K. & R. C. Donehower. Paclitaxel (taxol). N Engl J Med 1995;332:1004-14

40. Nakagawa T, Saitoh S, Imoto S, Itoh M, Tsutsumi M, Hikiji K, Nakao Y, Fujita T. Loss of multiple point mutations of RAS genes associated with acquisition of chromosomal abnormalities during disease progression in myelodysplastic syndrome. Br J Haematol. 1991;77(2):250-252.

41. Kitamura T, Tange T, Terasawa T, Chiba S, Kuwaki T, Miyagawa K, Piao YF, Miyazono K, Urabe A, Takaku F. Establishment and characterization of a unique human cell line that proliferates dependently on GM-CSF, IL-3, or erythropoietin. J Cell Physiol. 1989;140(2):323-334.

42. Matsuo Y, MacLeod RA, Uphoff CC, Drexler HG, Nishizaki C, Katayama Y, Kimura G, Fujii N, Omoto E, Harada M, Orita K. Two acute monocytic leukemia (AML-M5a) cell lines (MOLM-13 and MOLM-14) with interclonal phenotypic heterogeneity showing MLL-AF9 fusion resulting from an occult chromosome insertion, ins(11;9)(q23;p22p23). Leukemia. 1997;11(9):1469-1477.

43. Maimaitili Y, Inase A, Miyata Y, Kitao A, Mizutani Y, Kakiuchi S, Shimono Y, Saito Y, Sonoki T, Minami H, Matsuoka H.. An mTORC1/2 kinase inhibitor enhances the cytotoxicity of gemtuzumab ozogamicin by activation of lysosomal function. Leuk

Res. 2018;74:68-74.

44. Gururaja TL, Goff D, Kinoshita T, Goldstein E, Yung S, McLaughlin J, Pali E, Huang J, Singh R, Daniel-Issakani S, Hitoshi Y, Cooper RD, Payan DG. R-253 disrupts microtubule networks in multiple tumor cell lines. Clin Cancer Res. 2006 Jun 15;12(12):3831-42.

45. Thomas E, Gopalakrishnan V, Hegde M, Kumar S, Karki SS, Raghavan SC, Choudhary B. A novel resveratrol based tubulin inhibitor induces mitotic arrest and activates apoptosis in cancer cells. Sci Rep. 2016;6:34653.

46. Lee CH, Lin YF, Chen YC, Wong SM, Juan SH, Huang HM. MPT0B169 and MPT0B002, New Tubulin Inhibitors, Induce Growth Inhibition, G2/M Cell Cycle Arrest, and Apoptosis in Human Colorectal Cancer Cells. Pharmacology. 2018;102(5-6):262

47. Jackman RW, Rhoads MG, Cornwell E, Kandarian SC. Microtubule-mediated NF-kappaB activation in the TNF-alpha signaling pathway. Exp Cell Res. 2009;315(19):3242-3249.

48. Zeng QZ, Yang F, Li CG, Xu LH, He XH, Mai FY, Zeng CY, Zhang CC, Zha QB, Ouyang DY. Paclitaxel enhances the innate immunity by promoting NLRP3 inflammasome activation in macrophages. Front Immunol. 2019;10:72.

49. Mihara K, Chowdhury M, Nakaju N, Hidani S, Ihara A, Hyodo H, Yasunaga S, Takihara Y, Kimura A. Bmi-1 is useful as a novel molecular marker for predicting progression of myelodysplastic syndrome and patient prognosis. Blood. 2006;107(1):305-8

50. Harada Y, Harada H. Molecular pathways mediating MDS/AML with focus on AML1/RUNX1 point mutations. J Cell Physiol. 2009;220(1):16-20

51. Voncken JW, Schweizer D, Aagaard L, Sattler L, Jantsch MF, van Lohuizen M. Chromatin-association of the Polycomb group protein BMI1 is cell cycle-regulated and correlates with its phosphorylation status. J Cell Sci. 1999;112 (Pt 24):4627-39

52. Taga T, Shimomura Y, Horikoshi Y, Ogawa A, Itoh M, Okada M, Continuous and high-dose cytarabine combined chemotherapy in children with down syndrome and acute myeloid leukemia: Report from the Japanese children's cancer and leukemia study group (JCCLSG) AML 9805 down study. Pediatr Blood Cancer. 2011 Jul 15;57(1):36-40

53. Pavel Davidovich, Conor J Kearney, Seamus J Martin. Inflammatory Outcomes of Apoptosis, Necrosis and Necroptosis. Biol Chem. 2014;395(10):1163-71.

54. Yong Yang, Gening Jiang, Peng Zhang, Jie Fan. Programmed Cell Death and Its Role in Inflammation. Mil Med Res. 2015;2:12.

55. Jung YJ, Isaacs JS, Lee S, Trepel J, Neckers L. Microtubule disruption utilizes an NFkappa B-dependent pathway to stabilize HIF-1alpha protein. J Biol Chem. 2003;278(9):7445-52.

56. Kumuda C. Das, Carl W. White. Activation of NF-κB by antineoplastic agents. J Biol Chem. 1997;272:14914-14920.

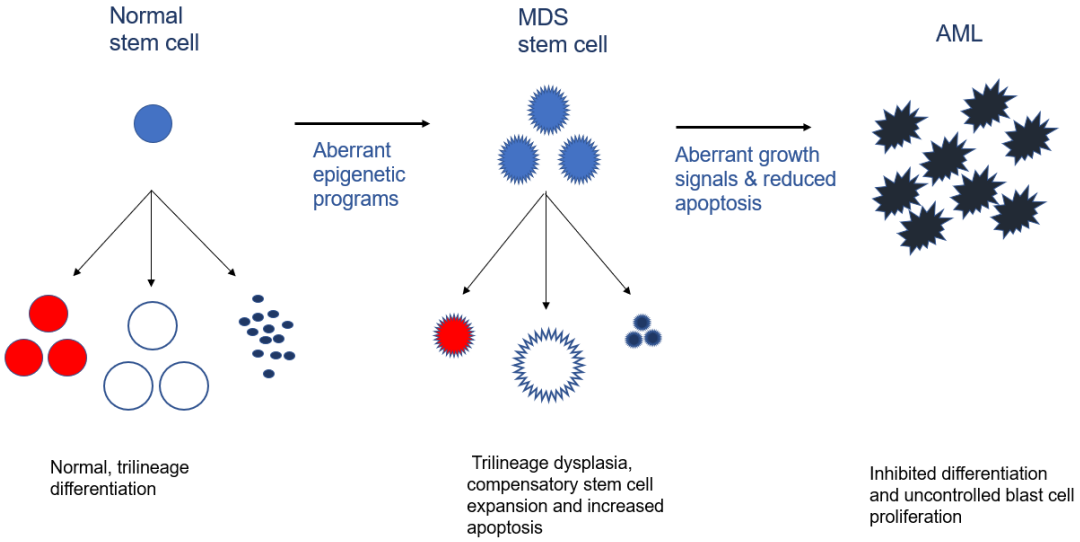

Figure 1 The process of clone evolution from normal stem cell to AML via MDS. Normal hematopoiesis is disrupted in MDS state before leukemogenesis.

Vincristine

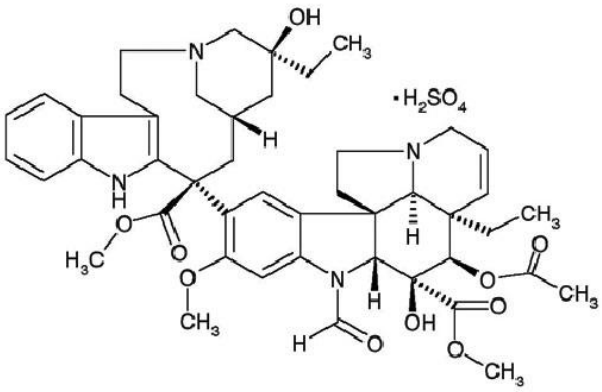

Paclitaxel

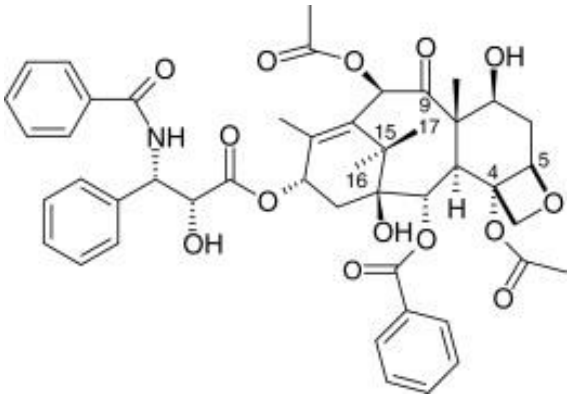

Figure 2 Chemical structure of clinically used microtubule inhibitors (Vincristine & Paclitaxel)

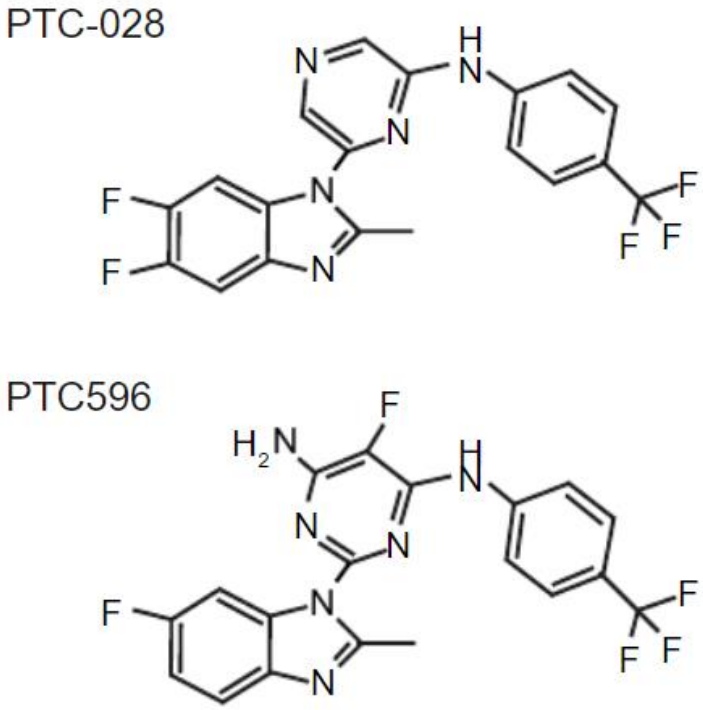

Figure 3 Chemical structure of PTC-028 and PTC596.

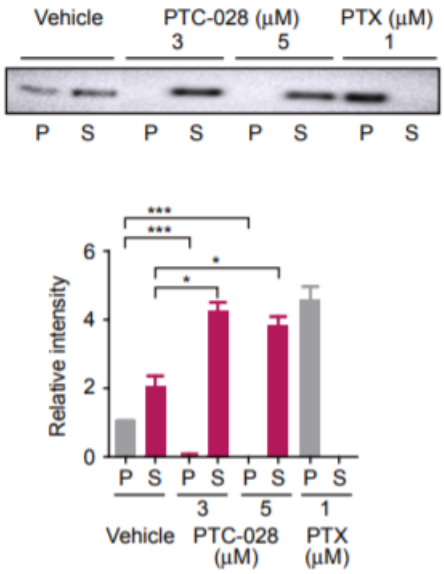

Figure 4 Distribution of tubulin in polymerized (P) vs. soluble (S) fractions analyzed by immunoblotting in PTC-028-treated MDS-L cells. MDS-L cells were treated with 3 and 5 μM of PTC-028 and 1 μM paclitaxel for 4 hours. The fractions containing soluble and polymerized tubulin were collected and separated by SDS-PAGE. The α-tubulin antibody was used to detect tubulin by Western blotting. Band intensity was calculated using Image lab (Bio-Rad) and was shown as means ± S.D. (n=3). *P<0.05, ***P<0.001 by the Student's *t*-test.

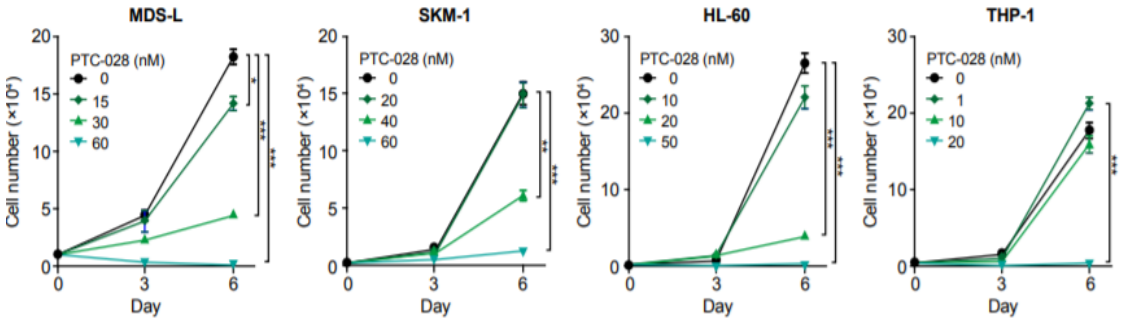

Figure 5 Growth of MDS-L and SKM-1 MDS cells and HL-60 and THP-1 AML cells treated with the indicated concentrations of PTC-028. The numbers of viable cells on days 3 and 6. Data are shown as means ± S.D. (n=3). *P<0.05, **P<0.01, ***P<0.001 by the Student's t-test.

Cell Line	CC50 (nM)
MDS-L (MDS)	40.3
SKM-1 (Monocytic leukemia from MDS)	78.6
MOLM-13 (Monocytic leukemia from MDS)	11.8
TF-1 (Erythroleukemia from MDS)	41.4
SKK-1 (Myeloid leukemia from MDS)	9.3
HL-60 (AML)	17.8
THP-1 (AML)	16.5

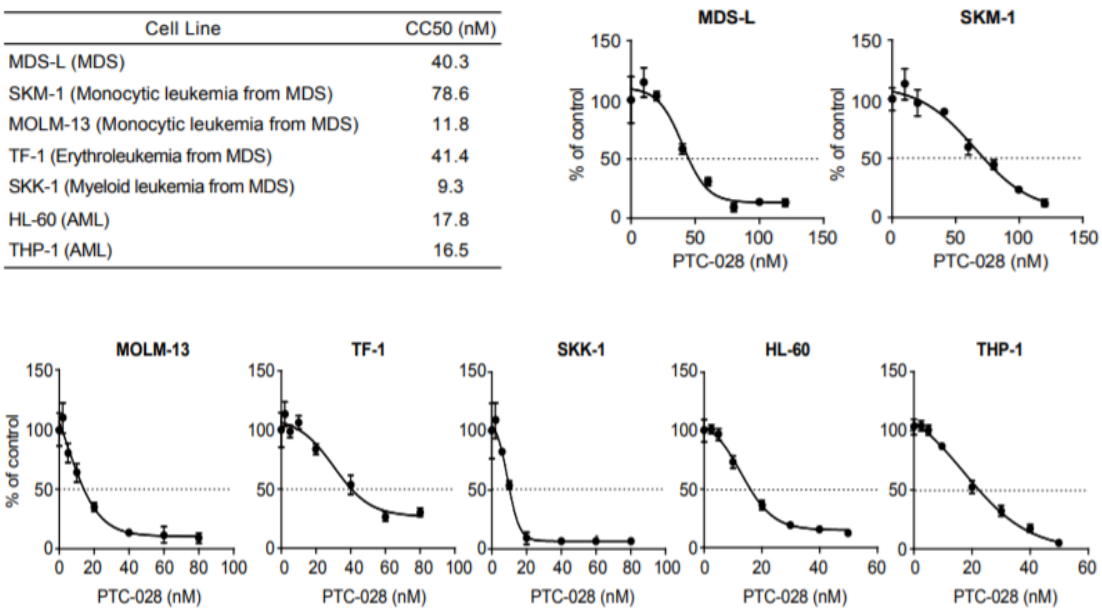

Figure 6 CC_{50} of MDS and AML cell lines. Cells lines were treated with the indicated concentrations of PTC-028 for 3 days in triplicate (left panels). CC_{50} was defined as the concentration required to reduce cell viability by 50% and is presented in the right panel. Cell viability was assessed by MTS assays.

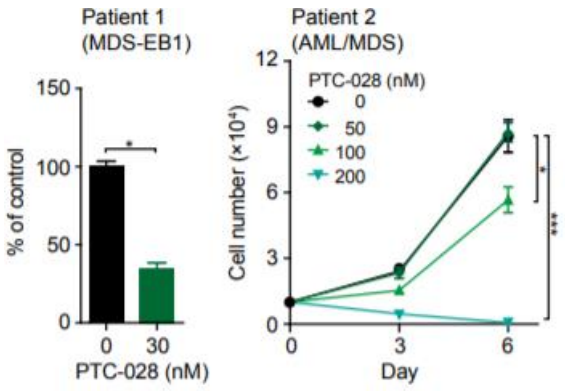

Figure 7 Growth of primary MDS cells treated with PTC-028. $CD34^+$ MDS cells were cultured in the presence of SCF, TPO, IL-3, GM-CSF, and FLT3 ligand in the presence of the indicated doses of PTC-028. Cell growth was examined by MTS assays after 48 hours in culture (left panel) or viable cells were counted on days 3 and 6 (right panel). Data are shown as means ± S.D. (n=3). *P<0.05, **P<0.01, ***P<0.001 by the Student's t-test.

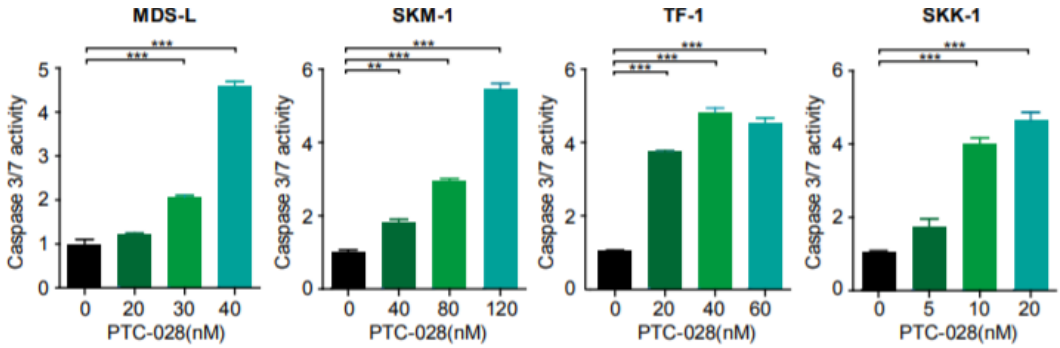

Figure 8 Caspase-Glo 3/7 values 3 days after the treatment with PTC-028. MDS cells were treated with PTC-028 at the indicated doses in triplicate. An equal volume of Caspase-Glo 3/7 agent was added to samples before recording luminescence. *P<0.05, **P<0.01, ***P<0.001 by the Student's *t*-test.

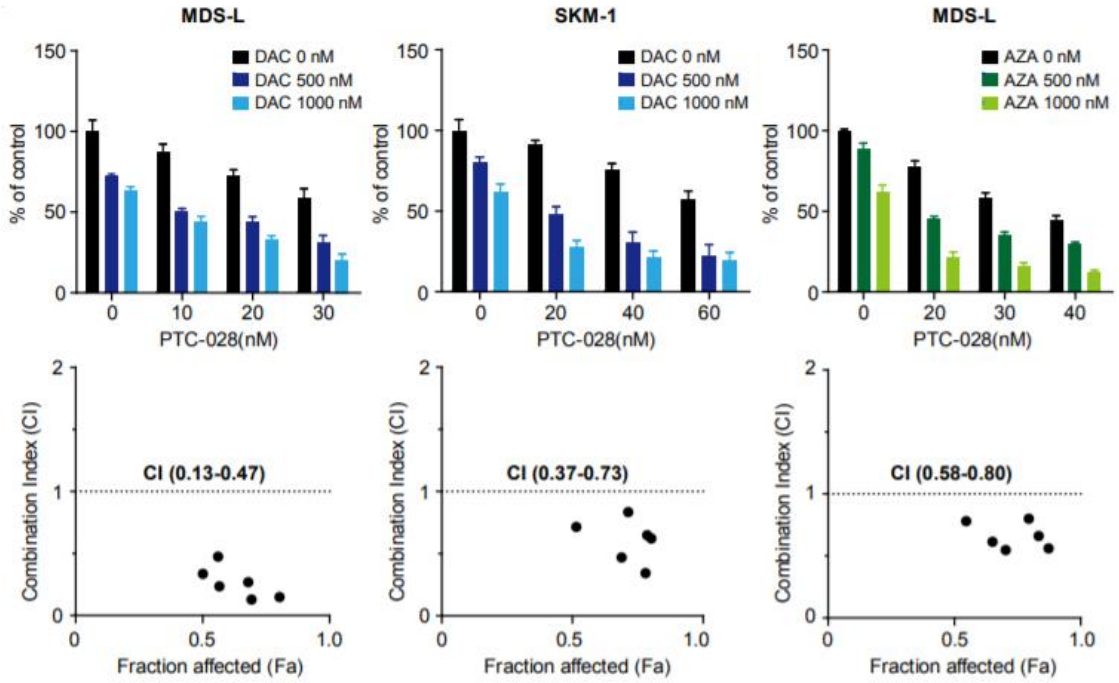

Figure 9 MTS assays showing the viability of MDS-L and SKM-1 cells treated with the indicated doses of PTC-028 and decitabine (DAC) or azacitidine (AZA) relative to the untreated control. Data are shown as means ± S.D. (n=3). Fa-CI plots are shown in the lower panel of each graph. CI, combination index. Fa (fraction affected) indicates the fraction of cells affected by the drug.

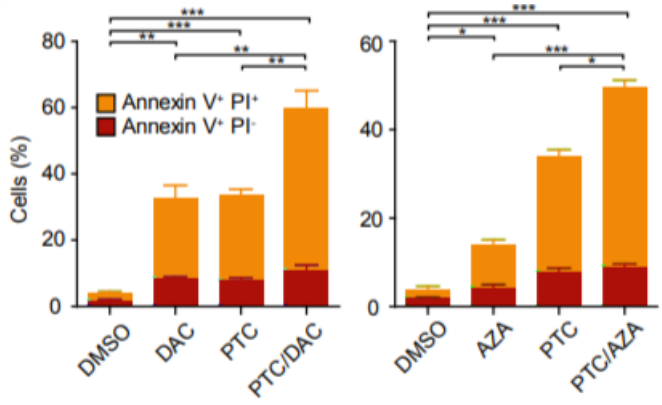

Figure 10 Apoptosis induced by PTC028 and/or DNA hypomethylating agents. MDS-L cells were treated with PTC-028 and/or DNA hypomethylating agents (DAC or AZA) for 72 hours, stained with Annexin V and PI, and then analyzed by flow cytometry. Results are shown as means ± S.D. (n=3). *P<0.05, **P<0.01, ***P<0.001 by the Student's *t*-test.

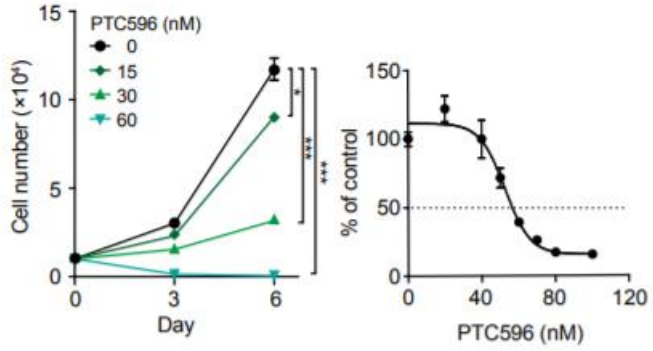

Figure 11 Growth inhibition of MDS-L cells by PTC596. Growth curve of MDS-L cells treated with the indicated concentrations of PTC596 (left panel) and CC_{50} of PTC596 in MDS-L cells (right panel). Cells were treated with the indicated concentrations of PTC596 for 3 days in triplicate to evaluate CC_{50}.

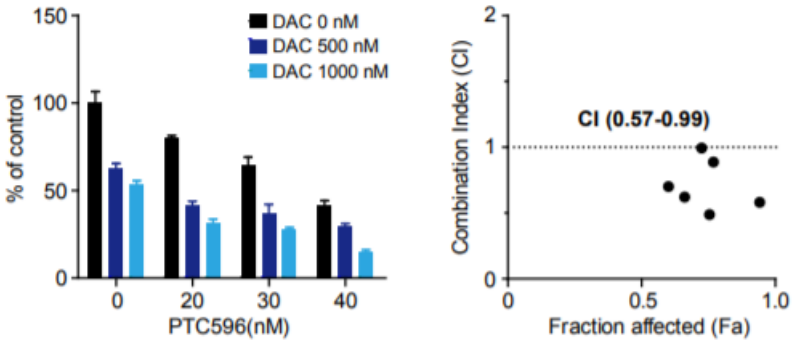

Figure 12 MTS assays showing the viability of MDS-L treated with the indicated doses of PTC596 and DAC relative to the untreated control (left panel) and a Fa-CI plot (right panel)

CC50 (nM)

Cell Line	PTC-028	PTC596	VCR	PTX
MDS-L (MDS)	38.5±7.6	52.3±9.8	93.7±10.6	>120.0
SKM-1 (MDS/AML)	80.8±9.5	91.0±8.3	>120.0	>120.0
HL-60 (AML)	17.8±4.6	18.4±5.9	>40.0	38.3±6.2
THP-1 (AML)	16.5±3.4	19.3±3.2	40.1±6.4	>50.0

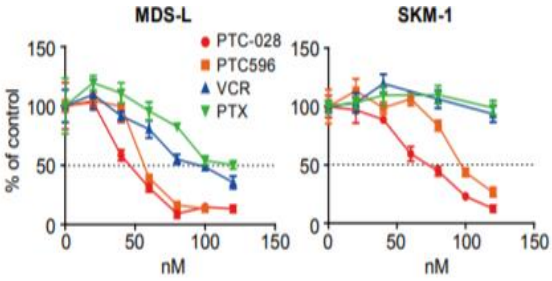

Figure 13 CC_{50} of microtubule-destabilizing agents in MDS and AML cells. Cell lines were treated with the indicated agents for 3 days in triplicate. Data are shown as means ± S.D. (n=3).

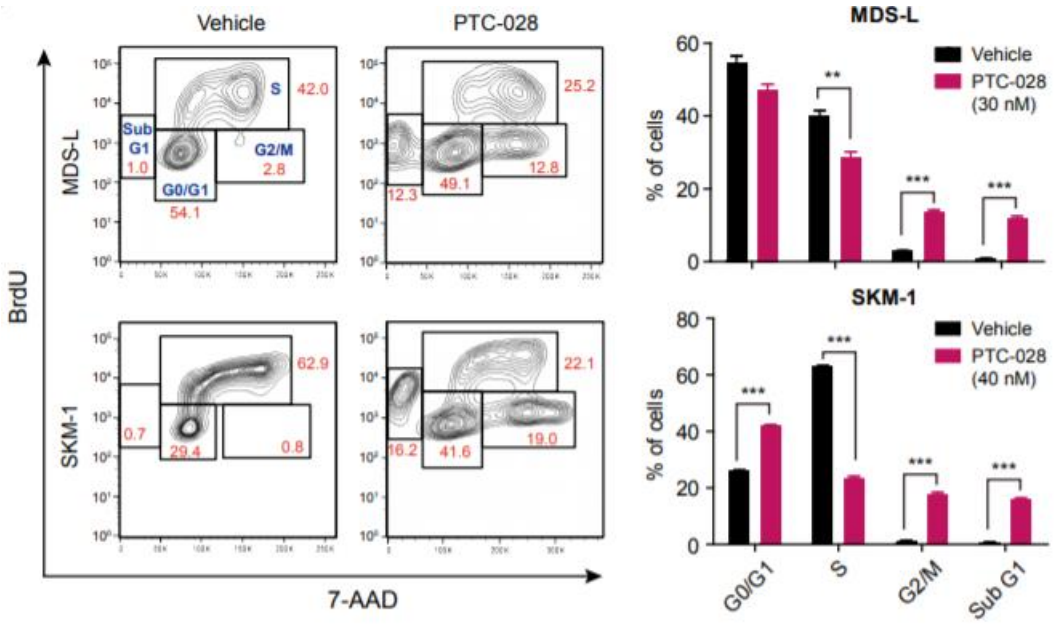

Figure 14 Cell cycle arrest induced by PTC-028. MDS-L and SKM-1 were exposed to PTC-028 for 72 hours at 40 and 80 nM, respectively. BrdU was added to the culture 4 hours before the analysis. Representative contour plots of BrdU incorporation (y axis) versus DNA content assessed by 7-AAD staining (x axis) are shown in the left panels. The proportion of cells at the indicated phase of the cell cycle is shown as means ± S.D. (n=3) in the right panels. **P<0.01, ***P<0.001 by the Student's *t*-test.

PTC-028

Gene Expression up

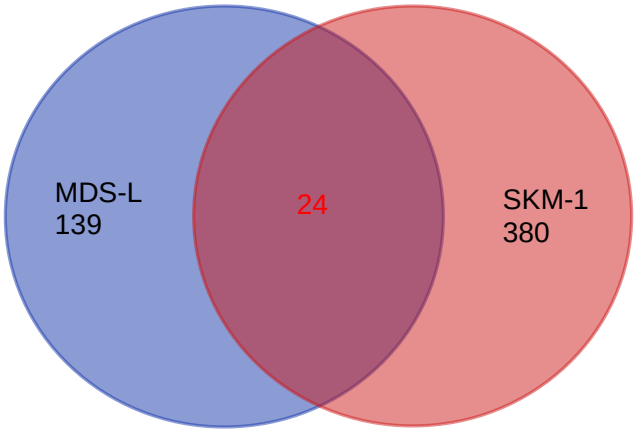

PTC-028

Gene Expression Down

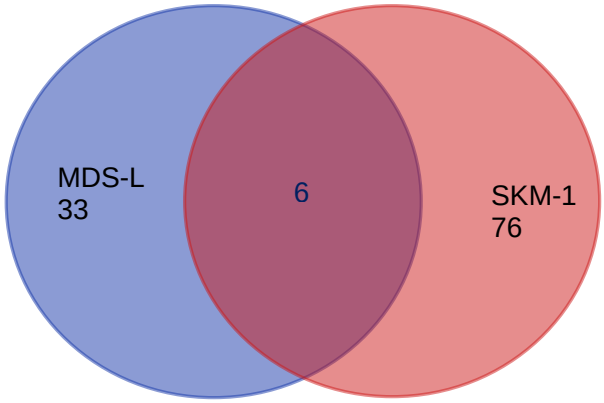

Figure 15 Venn diagram showing the overlap of up-regulated (≥1.5-fold) or down- (≤ 0.66-fold) genes between MDS-L and SKM-1 cells treated with PTC-028 relative to the DMSO control.

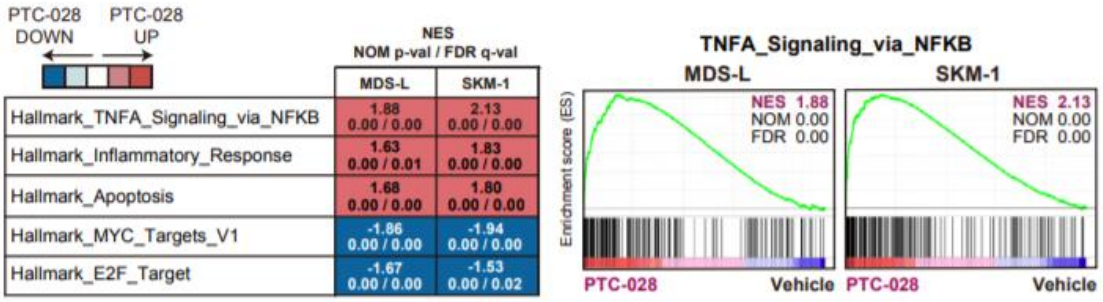

Figure 16 Summary of the gene set enrichment in MDS-L and SKM-1 cells treated with PTC-028 relative to non-treated cells in GSEA using RNA-seq data. MDS-L and SKM-1 cells were cultured in the presence of PTC-028 (MDS-L 30nM; SKM-1 40nM) for 72 hours. Representative GSEA plots are shown in the right panelspanels. Normalized enrichment scores (NES), nominal p values (NOM), and false discovery rates (FDR) are indicated.

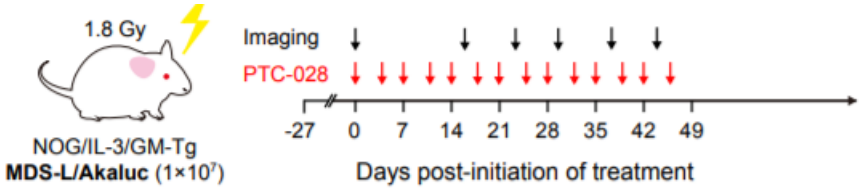

Figure 17 Schematic representation of the xenograft MDS model using NOG IL-3/GM-TG mice. NOG mice irradiated at a dose of 1.8 Gy were infused with 1×10^7 MDS-L/Akaluc cells via the tail vein. On day 27 post-transplantation, recipient mice (n=5 in each group) received vehicle and 12.5 mg/kg PTC-028 orally twice a week for 7 weeks.

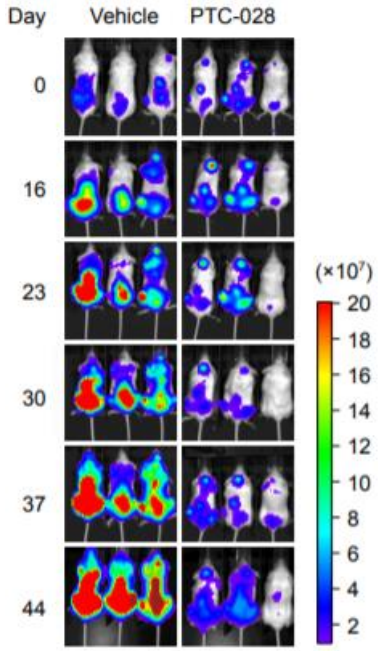

Figure 18 The engraftment of MDS-L/Akaluc cells was confirmed by bioluminescence imaging. Images of Akaluc signals in representative mice (3 mice each) are shown at different time points during the treatment.

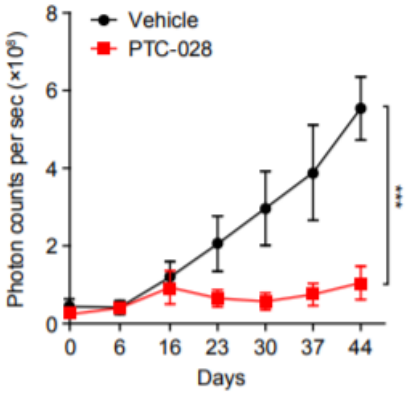

Figure 19 Quantification of photon counts from MDS-L/Akaluc cells in xenograft MDS mice. Akaluc signals taken by a photon-counting analyzer. Data are shown as means ± S.D. *P<0.05, **P<0.01, ***P<0.001 by the Student's *t*-test.

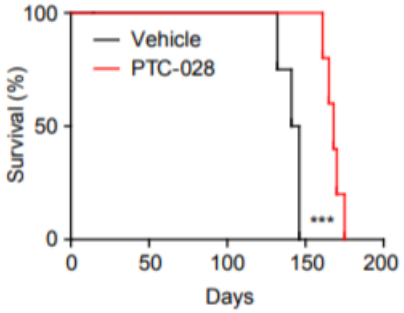

Figure 20 Kaplan–Meier survival of mice. Survival was evaluated from the first day of the treatment to death. The significance of differences between the PTC-028-treated and vehicle-treated groups was assessed using a Log-rank test. *P<0.05, **P<0.01, ***P<0.001.

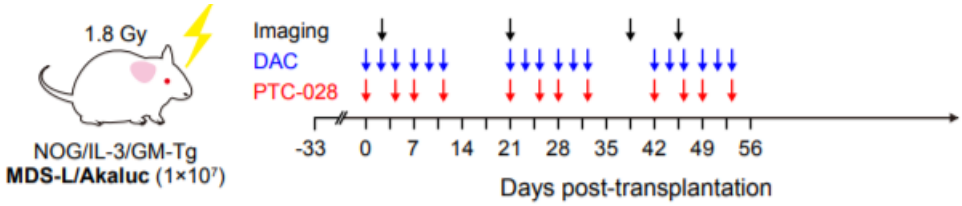

Figure 21 Schematic representation of the xenograft MDS model using NOG IL-3/GM-TG mice. NOG mice irradiated at a dose of 1.8 Gy were infused with 1×10^7 MDS-L/Akaluc cells via the tail vein. On day 33 post-transplantation, recipient mice (n=5 in each group) received vehicle and 6.25 mg/kg PTC-028 orally twice a week. DAC was administered at a dose of 0.3 mg/kg intraperitoneally 3 times per week.

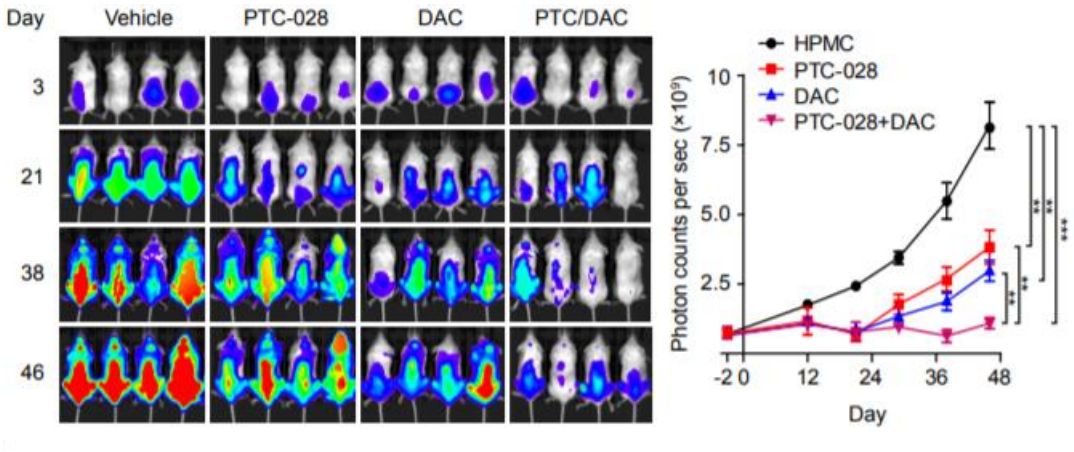

Figure 22 The engraftment of MDS-L/Akaluc cells was confirmed by bioluminescence imaging. Images of Akaluc signals in representative mice (4 mice each) are shown at different time points during the treatment. Quantification of photon counts from MDS-L/Akaluc cells in xenograft MDS mice. Akaluc signals taken by a photon-counting analyzer. Data are shown as means ± S.D. **P<0.01, ***P<0.001 by the Student's *t*-test.

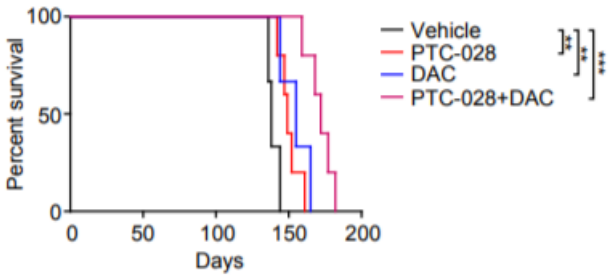

Figure 23 Kaplan–Meier survival of mice. Survival was evaluated from the first day of the treatment to death. **P<0.01, ***P<0.001 by the Log-rank test.

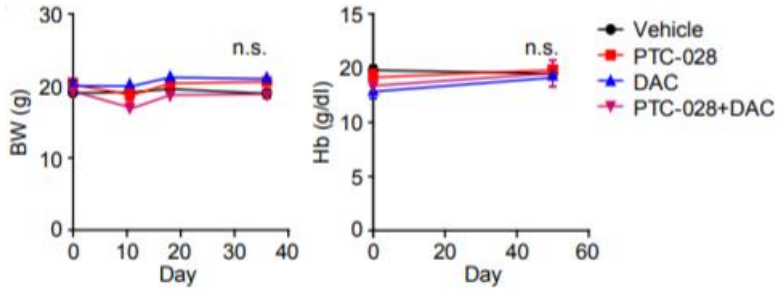

Figure 24 Body weight (BW) and hemoglobin (Hb) levels of mice. Data are shown as means ± S.D. n.s., not significant by the Student's *t*-test.

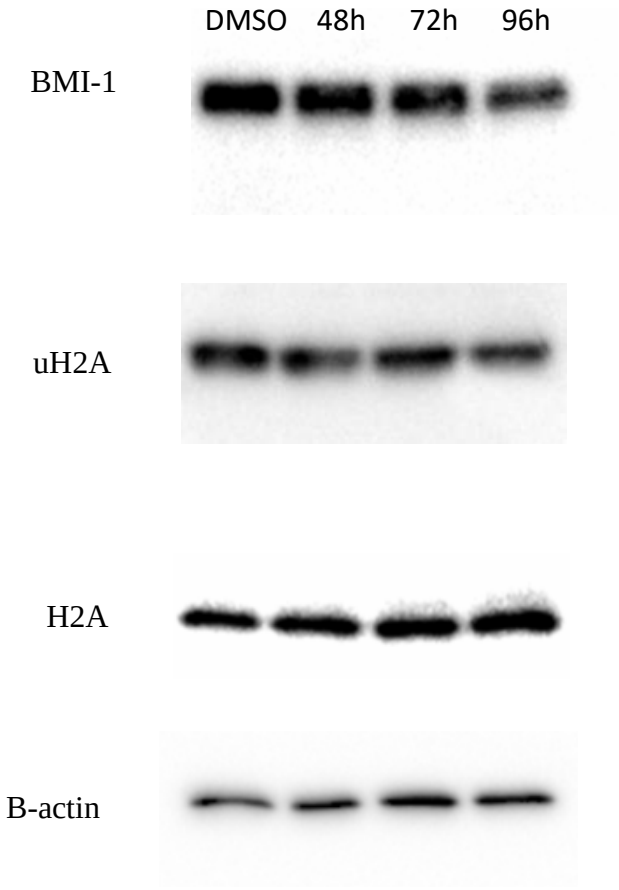

Figure 25 Level of BMI-1 and uH2A in MDS-L cells cultured in the presence of DMSO and 40nM PTC-028 for 48h, 72h and 96h.

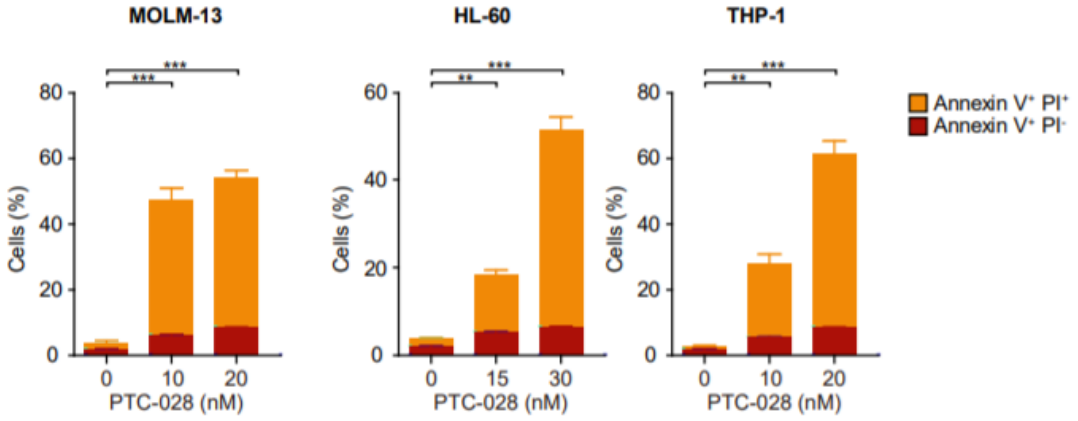

Figure 26. Apoptosis induced by PTC-028.The indicated cells were treated with PTC-028 for 72 hours, stained with Annexin V and PI, and then analyzed by flow cytometry. Results are shown as means ± S.D. (n=3). **P<0.01, ***P<0.001.

Table 1 Human MDS bone marrow samples.

	Patient 1	Patient 2
Sample	BM	BM
Diagnosis	MDS-EB1	MDS overt AML
Age	63	62
Sex	M	F
Blast (%)	3.3	46.8
Karyotype	Normal	Normal
WBC (/μl)	300	1700
Hb (g/dl)	6.8	8.5
MCV (fl)	87.1	84.0
PLT ($x10^4$ /μl)	1.8	2.9
R-IPSS	4.5	6
WT-1 mRNA (copy/μg RNA)	25534	840

Table 2 Upregulation of Signaling Pathway Induced by PTC-028 in MDS-L Cells

NAME	ES	NES	NOM p-val	FDR q-val
HALLMARK_TNFA_SIGNALING_VIA_NFKB	0.6108075	1.879353	0	0
HALLMARK_COAGULATION	0.5875037	1.7655075	0	0.002344156
HALLMARK_ALLOGRAFT_REJECTION	0.5704975	1.7577232	0	0.00187901
HALLMARK_P53_PATHWAY	0.54956275	1.7134482	0	0.00262637
HALLMARK_APOPTOSIS	0.54781187	1.6755384	0	0.004013803
HALLMARK_INTERFERON_GAMMA_RESPONSE	0.5385772	1.6667895	0	0.003868514
HALLMARK_INFLAMMATORY_RESPONSE	0.52368957	1.6260667	0	0.005695151
HALLMARK_IL6_JAK_STAT3_SIGNALING	0.55716753	1.579828	0.0013947	0.008902214
HALLMARK_INTERFERON_ALPHA_RESPONSE	0.55188423	1.5787069	0	0.008018492
HALLMARK_HEME_METABOLISM	0.5004975	1.5488061	0	0.009927
HALLMARK_IL2_STAT5_SIGNALING	0.48502183	1.5044812	0.001242236	0.016797332
HALLMARK_ANGIOGENESIS	0.5948357	1.4922953	0.033383913	0.01766459
HALLMARK_EPITHELIAL_MESENCHYMAL_TRANSITION	0.4732653	1.4622483	0.002528445	0.022271285
HALLMARK_UV_RESPONSE_DN	0.47187793	1.4172851	0.007692308	0.03291526
HALLMARK_BILE_ACID_METABOLISM	0.47735313	1.3960559	0.01899593	0.03932956
HALLMARK_COMPLEMENT	0.44702625	1.3827937	0.003911343	0.04317236
HALLMARK_ESTROGEN_RESPONSE_EARLY	0.42592376	1.3226221	0.011494253	0.080089346
HALLMARK_KRAS_SIGNALING_UP	0.410993	1.2768729	0.043209877	0.124076076

Table 3 Downregulation of Signaling Pathway Induced by PTC-028 in MDS-L Cells

NAME	ES	NES	NOM p-val	FDR q-val
HALLMARK_MYC_TARGETS_V1	-0.5312721	-1.8584391	0	0.004333333
HALLMARK_E2F_TARGETS	0.47660512	-1.6709709	0	0.005758667
HALLMARK_OXIDATIVE_PHOSPHORYLATION	-0.4207183	-1.5008153	0	0.029381553

Table 4 Upregulation of Signaling Pathway Induced by PTC-028 in SKM-1 Cells

NAME	ES	NES	NOM p-val	FDR q-val
HALLMARK_TNFA_SIGNALING_VIA_NFKB	0.6467109	2.1331067	0	0
HALLMARK_P53_PATHWAY	0.58609194	1.9506716	0	0
HALLMARK_APICAL_JUNCTION	0.58014596	1.9302019	0	0
HALLMARK_INFLAMMATORY_RESPONSE	0.55264056	1.8320497	0	2.87E-04
HALLMARK_APOPTOSIS	0.5546269	1.7967594	0	2.29E-04
HALLMARK_COAGULATION	0.55692613	1.7888622	0	1.91E-04
HALLMARK_MYOGENESIS	0.5327498	1.7650108	0	1.64E-04
HALLMARK_EPITHELIAL_MESENCHYMAL_TRANSITION	0.5172625	1.7131113	0	5.57E-04
HALLMARK_TGF_BETA_SIGNALING	0.5863241	1.6650617	0	0.002022102
HALLMARK_IL6_JAK_STAT3_SIGNALING	0.5481379	1.661659	0	0.001819892
HALLMARK_HYPOXIA	0.49732518	1.6503032	0	0.002014123
HALLMARK_NOTCH_SIGNALING	0.6159639	1.5805967	0.014059754	0.005915025
HALLMARK_ALLOGRAFT_REJECTION	0.47112146	1.5666751	0	0.00652423
HALLMARK_ANGIOGENESIS	0.6000284	1.5502645	0.014876033	0.00710283
HALLMARK_UV_RESPONSE_UP	0.47220153	1.522929	0	0.008662837
HALLMARK_IL2_STAT5_SIGNALING	0.45630616	1.5213256	0	0.008390245
HALLMARK_KRAS_SIGNALING_UP	0.45659617	1.5073739	0.001416431	0.009566529
HALLMARK_XENOBIOTIC_METABOLISM	0.4333904	1.4450694	0	0.017967768
HALLMARK_INTERFERON_GAMMA_RESPONSE	0.43104485	1.4400431	0.001369863	0.018887723
HALLMARK_COMPLEMENT	0.43133524	1.4359385	0.005479452	0.018809563
HALLMARK_REACTIVE_OXIGEN_SPECIES_PATHWAY	0.5228781	1.4232961	0.031045752	0.021028811

Table 5 Downregulation of Signaling Pathway Induced by PTC-028 in SKM-1 Cells

NAME	ES	NES	NOM p-val	FDR q-val
HALLMARK_MYC_TARGETS_V1	0.53554523	-1.9443746	0	0
HALLMARK_E2F_TARGETS	0.42601994	-1.5342134	0	0.022642275
HALLMARK_PROTEIN_SECRETION	0.46719083	-1.5294216	0.002890173	0.01509485
HALLMARK_ANDROGEN_RESPONSE	0.40367532	-1.3367312	0.017045455	0.07223807